

Activities in the Spinel Solid Solution $\text{Fe}_x\text{Mg}_{1-x}\text{Al}_2\text{O}_4$

K.T. JACOB and RASHMI PATIL

Activities in the spinel solid solution $\text{Fe}_x\text{Mg}_{1-x}\text{Al}_2\text{O}_4$ saturated with $\alpha\text{-Al}_2\text{O}_3$ have been measured for the compositional range $0 < X < 1$ between 1100 and 1350 K using a bielectrolyte solid-state galvanic cell, which may be represented as Pt, Fe + $\text{Fe}_x\text{Mg}_{1-x}\text{Al}_2\text{O}_4$ + $\alpha\text{-Al}_2\text{O}_3$ // $(\text{Y}_2\text{O}_3)\text{ThO}_2$ / $(\text{CaO})\text{ZrO}_2$ // Fe + FeAl_2O_4 + $\alpha\text{-Al}_2\text{O}_3$, Pt. Activities of ferrous and magnesium aluminates exhibit small negative deviations from Raoult's law. The excess free energy of mixing of the solid solution is a symmetric function of composition and is independent of temperature: $\Delta G^E = -1990 X(1 - X)$ J/mol. Theoretical analysis of cation distribution in spinel solid solution also suggests mild negative deviations from ideality. The lattice parameter varies linearly with composition in samples quenched from 1300 K. Phase relations in the FeO-MgO- Al_2O_3 system at 1300 K are deduced from the results of this study and auxiliary thermodynamic data from the literature. The calculation demonstrates the influence of intracrystalline ion exchange equilibrium between nonequivalent crystallographic sites in the spinel structure on intercrystalline ion exchange equilibrium between the monoxide and spinel solid solutions (tie-lines). The composition dependence of oxygen partial pressure at 1300 K is evaluated for three-phase equilibria involving the solid solutions Fe + $\text{Fe}_x\text{Mg}_{1-x}\text{Al}_2\text{O}_4$ + $\alpha\text{-Al}_2\text{O}_3$ and Fe + $\text{Fe}_y\text{Mg}_{1-y}\text{O}$ + $\text{Fe}_x\text{Mg}_{1-x}\text{Al}_2\text{O}_4$. Dependence of X , denoting the composition of the spinel solid solution, on parameter Y , characterizing the composition of the monoxide solid solution with rock salt structure, in phase fields involving the two solid solutions is elucidated. The tie-lines are slightly skewed toward the MgAl_2O_4 corner.

I. INTRODUCTION

SPINEL (*sensu stricto*, MgAl_2O_4) and hercynite (FeAl_2O_4) are two very common minerals in the spinel series.^[1] The compositions of many natural spinels range from pure MgAl_2O_4 through pleonaste (Mg:Fe ratio varying between 3 to 1) to nearly pure FeAl_2O_4 . This observation suggests a continuous solid solution between MgAl_2O_4 and FeAl_2O_4 . Such spinel solid solutions have been widely reported from contact metamorphosed marble^[2,3] argillaceous metasediments,^[4] analcime basanites,^[5] alkalic trachybasalts,^[6] ultrabasic rocks,^[7] and mantle xenoliths and xenocrysts.^[8,9]

As the spinel solid solution $\text{Fe}_x\text{Mg}_{1-x}\text{Al}_2\text{O}_4$ contains iron (a transition metal) in its lower valent state, its stability and chemistry are dependent on f_{O_2} - T conditions associated with their formation. Thus, detailed knowledge of phase equilibria in the system FeO-MgO- Al_2O_3 at high temperatures and the determination of activities in the spinel solid solution and chemical potentials corresponding to three-phase equilibria have important bearing on the genesis of rocks containing such spinels. These data are also useful for analysis of slag-refractory interactions in pyrometallurgical processing. As part of a larger program of research on thermodynamic properties of spinel solid solutions in general, activities in the $\text{Fe}_x\text{Mg}_{1-x}\text{Al}_2\text{O}_4$ solid solution have been measured using a solid-state galvanic cell. Excess free energies of mixing of the spinel solutions at 1300 K have been evaluated and compared with theoretical calculations.

An isothermal section of the system FeO-MgO- Al_2O_3 at 1300 K has been computed.

II. EXPERIMENTAL TECHNIQUE

A. Materials

Hercynite and spinel (*sensu stricto*) were prepared by heating pellets of Fe + Fe_2O_3 + Al_2O_3 and MgO + Al_2O_3 , respectively, in the required molar ratios at 1400 K for 6 days. The pellets were contained in alumina crucibles sealed inside evacuated silica capsules. The purity of the starting materials was better than 99.99 pct. Alumina powder used for synthesis was obtained by vacuum decomposition of $\text{Al}_2(\text{SO}_4)_3$. This material was found to be mainly amorphous and highly reactive. Hercynite synthesized in this study had a light bluish-green color. Spinel solid solutions were prepared by the same method used for synthesizing pure spinels; however, after the initial heat treatment, the material was crushed, repelletized, resealed, and equilibrated at 1400 K for an additional 6 days. The formation of spinel compounds and homogeneous solid solutions was confirmed by X-ray diffraction (XRD). The variation of the lattice parameter with composition of the solid solution quenched from 1300 K is shown in Figure 1. Within experimental uncertainty, the lattice parameter is found to vary linearly with composition:

$$a = 0.80841 + 0.00676X (\pm 0.00013) \text{ nm} \quad [1]$$

The argon gas used to provide an inert atmosphere over the electrodes of the cell was 99.999 pct pure and was further dried by passing through columns containing anhydrous magnesium perchlorate and phosphorus pentoxide. The gas was then deoxidized by passing through columns of copper wool kept at 873 K and titanium granules at 1200 K.

K.T. JACOB, Professor, is with the Department of Metallurgy and Materials Research Centre, Indian Institute of Science, Bangalore-560 012, India. RASHMI PATIL, Short-Term Fellow of Indian Academy of Sciences at Department of Metallurgy, Indian Institute of Science, is from the Department of Chemical Engineering, Karnataka Regional Engineering College, Surathkal 574 157, India.

Manuscript submitted September 24, 1997.

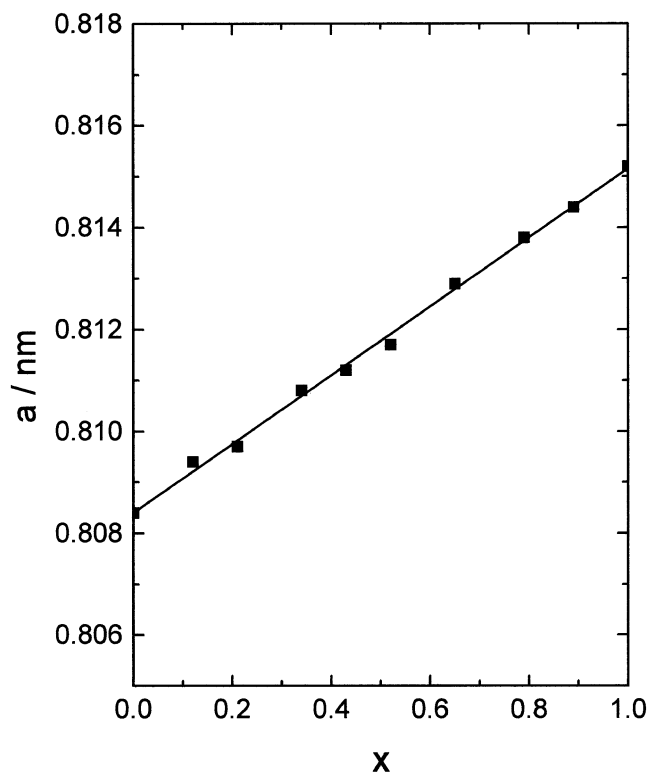


Fig. 1—Variation of lattice parameter (a) with composition (X) of the spinel solid solution $\text{Fe}_x\text{Mg}_{1-x}\text{Al}_2\text{O}_4$. The samples were quenched from 1300 K.

B. Apparatus and Procedure

The reversible electromotive force (emf) of the cell, Pt, Fe + $\text{Fe}_x\text{Mg}_{1-x}\text{Al}_2\text{O}_4 + \alpha\text{-Al}_2\text{O}_3 // (\text{Y}_2\text{O}_3)\text{ThO}_2 / (\text{CaO})\text{ZrO}_2 / \text{Fe} + \text{FeAl}_2\text{O}_4 + \alpha\text{-Al}_2\text{O}_3$, Pt was measured as a function of temperature. The apparatus used for measurements was similar to that described earlier.^[10] A stabilized zirconia tube, containing 15 mol pct CaO, was used to separate the gas phase over the reference electrode from that over the measuring electrode. This construction minimizes oxygen transport between the two electrodes *via* the gas phase. The bioelectrolyte cell was arranged in such a way that the $(\text{Y}_2\text{O}_3)\text{ThO}_2$ electrolyte was adjacent to the measuring electrode containing the spinel solid solution. The use of doped-thoria electrolyte near the low oxygen potential electrode ensures that the oxygen transport number is unity for the solid electrolyte combination. Separate streams of prepurified argon gas were passed over each electrode.

The electrode pellets contained an equimolar mixture of iron, spinel phase, and α -alumina and were sintered at 1400 K under argon prior to incorporation in the cell. The electrode pellets were held tightly against the solid electrolytes by a system of spring-loaded alumina tubes and slabs. The springs were attached to a water-cooled brass head capping the top of the outer alumina tube. Temperature of the cell was measured by a Pt/Pt-13 pct Rh thermocouple placed 3 mm below the reference electrode. The thermocouple was checked against the melting point of gold.

The emf of the cell was measured with a digital voltmeter with an internal impedance greater than 10^{12} ohms. The emf was independent of the flow rate of argon gas over the electrodes. The emfs became constant in 3 to 8 hours after

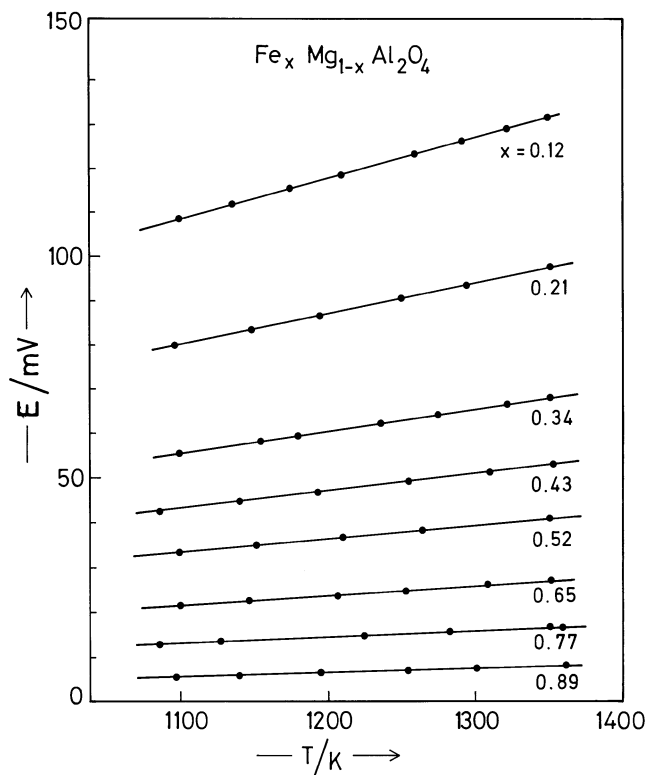


Fig. 2—Variation of emf of the electrochemical cell with temperature for different compositions of the spinel solid solution.

stabilization of temperature. The reversibility of the cell was checked by passing small currents ($\sim 100 \mu\text{A}$ for 3 minutes) through the cell in either direction using an external potential source, and ensuring that the emf after each coulometric titration returned to the same value. The emfs were reproducible (± 0.2 mV) after temperature cycling. To ensure the absence of stray contributions to the emf generated, for example, by thermal gradients across the solid electrolyte, a symmetric cell was assembled with identical electrodes on either side of the solid electrolyte. The voltage of this cell was ± 0.15 mV and varied randomly on changing temperature.

After the emf measurements, electrode pellets were equilibrated at 1300 K for 16 hours in evacuated silica capsules and quenched in liquid nitrogen. The composition of larger spinel grains (diameter $> 30 \mu\text{m}$) was determined by electron microprobe using energy dispersive X-ray analysis. Dense pellets of pure MgO , Al_2O_3 , and Fe_2O_3 were used as standards. In all cases, atomic absorption and fluorescence effects were eliminated using computer-compensated adjustments (ZAF). Composition profiles across the grains were found to be uniform. Excess alumina in the spinel phase saturated with α -alumina is $1.5 (\pm 0.5)$ mol pct in pure MgAl_2O_4 and it decreases to ~ 0.8 mol pct in pure FeAl_2O_4 at 1300 K. The solubility is small enough to be neglected.

III. RESULTS

The reversible emfs obtained as a function of temperature for eight spinel compositions are plotted in Figure 2. Within experimental uncertainty, the emfs can be represented by

Table I. Summary of Experimental Results

X	E/mV (± 0.2)	$a_{FeAl_2O_4}$ (1300 K)	$\Delta H_{FeAl_2O_4}/$ $J mol^{-1}$	Ω/J mol^{-1}
0.12	$7.78 + 9.12 \times 10^{-2} T$	0.105	-1500	-1937
0.21	$6.08 + 6.72 \times 10^{-2} T$	0.189	-1173	-1860
0.34	$4.36 + 4.64 \times 10^{-2} T$	0.315	-841	-1932
0.43	$3.06 + 3.64 \times 10^{-2} T$	0.407	-590	-1817
0.52	$2.50 + 2.80 \times 10^{-2} T$	0.499	-483	-2094
0.65	$1.36 + 1.84 \times 10^{-2} T$	0.637	-263	-2147
0.77	$0.58 + 1.12 \times 10^{-2} T$	0.763	-112	-2116
0.89	$0.42 + 4.80 \times 10^{-3} T$	0.888	-81	(-6694)*
1.00	0	1.000	0	($\Omega_{av} = -1990$)

*Value ignored in the calculation of Ω_{av} .

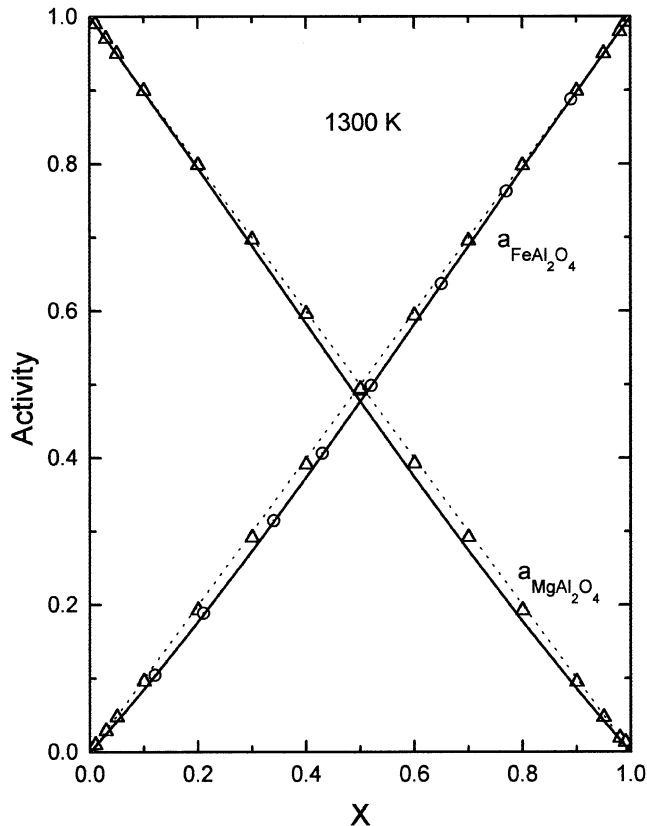
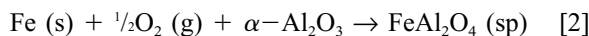


Fig. 3—Activities in the spinel solid solution $Fe_xMg_{1-x}Al_2O_4$ at 1300 K: Δ computed from cation distribution; \circ — experimental data; and ---- Raoult's law.

linear equations. The coefficients of linear equations obtained by least-mean-squares regression analysis are summarized in Table I. The oxygen potential at the electrodes is established by the reaction



Since Fe and Al_2O_3 are present at unity activity, the oxygen partial pressure (P_{O_2}) is related to the equilibrium constant (K_2) for the reaction and the activity of ferrous aluminate:

$$P_{O_2}^{1/2} = a_{FeAl_2O_4}/K_2 \quad [3]$$

By choosing ferrous aluminate saturated with α -alumina as the standard state, the activity of hercynite in the reference electrode is set at unity. The emf (E) of cell I is related

to the difference in oxygen partial pressure at the two electrodes:

$$E = (RT/2F) \ln [P_{O_2}^{1/2}(ref)/P_{O_2}^{1/2}(ss)] \quad [4]$$

where $P_{O_2}(ss)$ is the oxygen partial pressure established by the electrode containing the spinel solid solution, $P_{O_2}(ref)$ is the oxygen partial pressure at the reference electrode, F is the Faraday constant, and the other symbols have their usual meaning. Combining Eqs. [3] and [4],

$$E = -(RT/2F) \ln a_{FeAl_2O_4} \quad [5]$$

The activity of ferrous aluminate calculated using this equation at 1300 K is given in Table I. The activities exhibit small negative deviations from Raoult's law, as shown in Figure 3. The activity of magnesium aluminate derived using the Gibbs–Duhem equation is also plotted as a function of composition in the figure. The relative partial enthalpy of nonstoichiometric ferrous aluminate in the solid solution, calculated from the emf using the relation,

$$\Delta H_{FeAl_2O_4} = -2FE + 2FT(dE/dT) \quad [6]$$

is also given in Table I. The relative partial molar entropy of ferrous aluminate calculated from emf,

$$\Delta S_{FeAl_2O_4} = 2F(dE/dT) \quad [7]$$

is found to be close to the ideal value ($-R \ln X$), except for $X = 0.89$. Since the emf corresponding to this composition is small, error in the calculated partial entropy is large.

Ignoring this composition, the regular solution parameter,

$$\Omega = \frac{\Delta H_{FeAl_2O_4}}{X(1-X)} \quad [8]$$

is found to be approximately constant and independent of composition, as shown in Table I. The average value is $-1990(\pm 170)$ J/mol. Therefore, the thermodynamic mixing properties can be represented as

$$\Delta H = \Delta G^E = -1900X(1-X) \text{ J/mol} \quad [9]$$

where ΔH and ΔG^E are the integral enthalpy and excess free energy of mixing of the solid solution. Since entropy of mixing is almost ideal [$\Delta S = -R(X \ln X + (1-X) \ln(1-X))$], the excess free energy is independent of temperature.

IV. THEORETICAL CALCULATION

The activity-composition relationship in stoichiometric spinel solid solutions can be calculated from a knowledge of cation distribution between tetrahedral and octahedral sites of the spinel structure. Ion exchange equilibria between these sites is governed by site preference energies of cations, as discussed by Jacob and Alcock.^[11] At low temperature, $MgAl_2O_4$ is a normal spinel. However, there is significant disorder at elevated temperatures. The cation distribution in $MgAl_2O_4$ has been measured as a function of temperature by three groups of investigators using magic-angle spinning nuclear magnetic resonance (MAS NMR)^[12,13] and neutron diffraction^[14] techniques. Results of Millard *et al.*^[13] are more reliable than those of Wood *et*

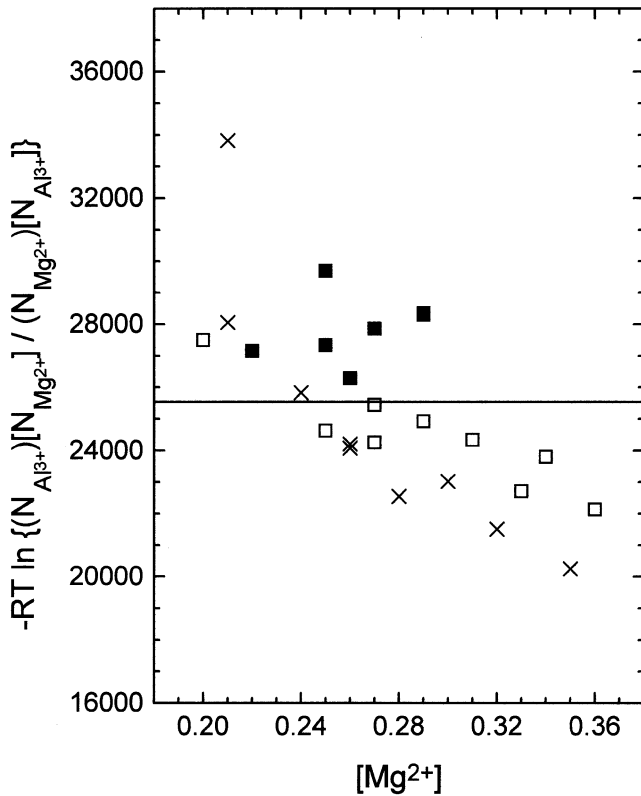
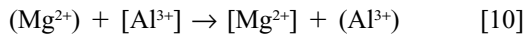


Fig. 4—Variation of the function $-RT \ln \{(N_{Al^{3+}})[N_{Mg^{2+}}]/(N_{Mg^{2+}})[N_{Al^{3+}}]\}$ with $[N_{Mg^{2+}}]$ for $MgAl_2O_4$. Data are from Wood *et al.*,^[12] X; Millard *et al.*,^[13] ■; and Peterson *et al.*,^[14] □.

al.,^[12] since the former used more appropriate instrument parameters for acquisition of ^{27}Al MAS NMR spectra. Below 900 K, ion exchange between sites is very slow and equilibrium distribution is not attained in the timeframe of laboratory experiments. Equilibrium cation distribution above 1273 K cannot be quenched. The cation distribution is determined by the ion exchange reaction:^[11]



where the parentheses denote tetrahedral and the brackets represent octahedral sites, respectively.

Assuming ideal mixing of cations on both sites, negligible standard entropy change for the exchange reaction, and octahedral site preference energies independent of composition, the ion exchange equilibria can be quantified by the relation^[11]

$$\Delta H^{ex} = H_{Mg^{2+}}^o - H_{Al^{3+}}^o = -RT \ln \frac{(N_{Al^{3+}})[N_{Mg^{2+}}]}{(N_{Mg^{2+}})[N_{Al^{3+}}]} \quad [11]$$

where (N_i) and $[N_i]$ represent ionic fractions in the tetrahedral and octahedral sites, respectively; and $H_{Mg^{2+}}^o$ and $H_{Al^{3+}}^o$ are the octahedral site preference energies of Mg^{2+} and Al^{3+} ions, respectively. A test of Eq. [11] using temperature dependence of measured cation distribution in pure $MgAl_2O_4$ is provided in Figure 4. The right-hand side of Eq. [11] should be independent of the concentration of Mg^{2+} ion on octahedral site, $[Mg^{2+}]$. Experimental data show a decrease. Such behavior has been attributed by O'Neill and Navrotsky^[15] to a quadratic dependence of the

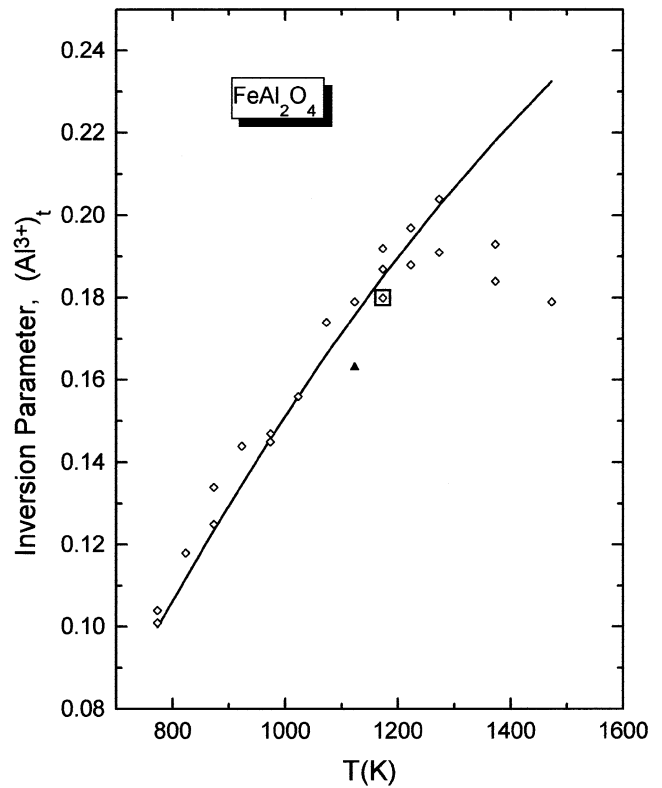
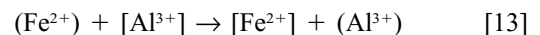


Fig. 5—Comparison of experimental data on cation distribution in $FeAl_2O_4$ with Eq. [14]. $(Al^{3+})_t$ represents ionic fraction of Al^{3+} on tetrahedral site. \diamond Larsson *et al.*,^[17] \blacktriangle Hill,^[18] and \square Bohlen *et al.*^[19]

enthalpy of disordering on the cation distribution parameter. Electrostatic considerations were invoked^[15] to justify the quadratic dependence. Iyengar *et al.*^[16] have recently shown that if enthalpy of mixing of ions on tetrahedral and octahedral sites are incorporated in the framework of the regular solution model, one obtains an equation very similar to that proposed by O'Neill and Navrotsky.^[15] In both the models, the quantity on the right-hand side of Eq. [11] would be a linear function of $[Mg^{2+}]$. However, in view of the scatter in the data, an average value is chosen, independent of cation disorder or temperature. The cation distribution in $MgAl_2O_4$ is then represented by

$$-RT \ln \frac{(N_{Al^{3+}})[N_{Mg^{2+}}]}{(N_{Mg^{2+}})[N_{Al^{3+}}]} = 25,540 \text{ J/mol} \quad [12]$$

The cation distribution in $FeAl_2O_4$ has been measured in the temperature range 773 to 1473 K by Larsson *et al.*^[17] using Rietveld refinement of an XRD powder pattern of quenched samples. Similar studies have been conducted by Hill^[18] at 1123 K and Bohlen *et al.*^[19] at 1173 K. It was difficult to quench equilibrium cation distribution in samples heat treated above 1300 K. The ion exchange between sites can be represented by the equation



for which

$$\Delta H^{ex} = 26,000 = -RT \ln \frac{(N_{Al^{3+}})[N_{Fe^{2+}}]}{(N_{Fe^{2+}})[N_{Al^{3+}}]} - RT \ln 3 \quad [14]$$

Table II. Computed Cation Distribution and Activities in $\text{Fe}_x\text{Mg}_{1-x}\text{Al}_2\text{O}_4$ Spinel Solid Solution at 1300 K

X	Ionic Fraction of Cations						$a_{\text{FeAl}_2\text{O}_4}$	$a_{\text{MgAl}_2\text{O}_4}$
	Tetrahedral			Octahedral				
	$(N_{\text{Fe}^{2+}})$	$(N_{\text{Mg}^{2+}})$	$(N_{\text{Al}^{3+}})$	$[N_{\text{Fe}^{2+}}]$	$[N_{\text{Mg}^{2+}}]$	$[N_{\text{Al}^{3+}}]$		
0.0	—	0.6741	0.3259	—	0.1630	0.8370	0.000	1.000
0.1	0.0862	0.5987	0.3151	0.0069	0.1507	0.8425	0.0960	0.8997
0.2	0.1713	0.5246	0.3041	0.0144	0.1377	0.8480	0.1932	0.7987
0.3	0.2552	0.4519	0.2929	0.0224	0.1241	0.8536	0.2916	0.6971
0.4	0.3379	0.3809	0.2812	0.0311	0.1096	0.8594	0.3914	0.5957
0.5	0.4190	0.3116	0.2694	0.0405	0.0942	0.8653	0.4920	0.4940
0.6	0.4985	0.2443	0.2572	0.0508	0.0779	0.8714	0.5937	0.3928
0.7	0.5759	0.1792	0.2449	0.0621	0.0604	0.8776	0.6955	0.2922
0.8	0.6511	0.1165	0.2324	0.0745	0.0418	0.8838	0.7976	0.1927
0.9	0.7236	0.0567	0.2197	0.0882	0.0217	0.8902	0.8992	0.0951
1.0	0.7931	—	0.2069	0.1034	—	0.8966	1.000	0.000

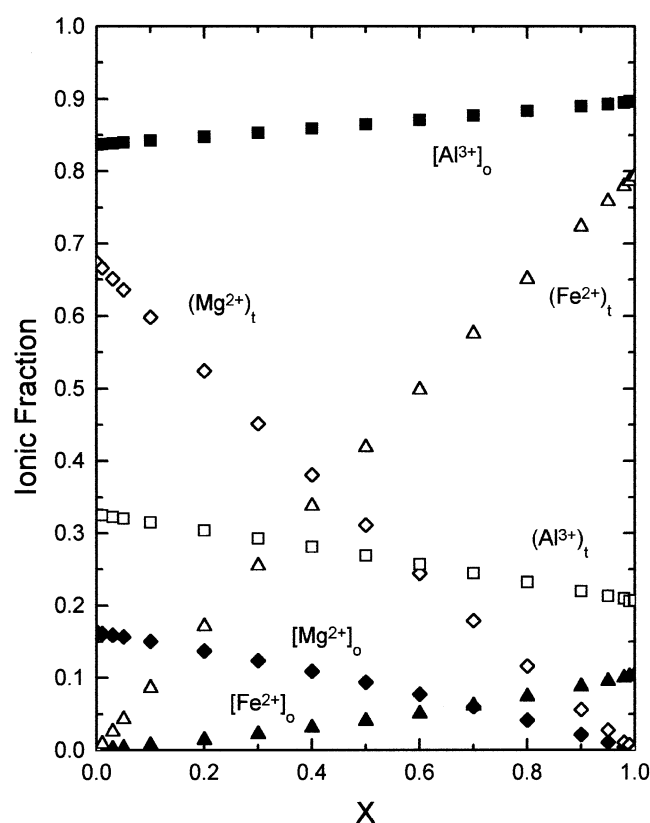


Fig. 6—Computed cation distribution between tetrahedral and octahedral sites of $\text{Fe}_x\text{Mg}_{1-x}\text{Al}_2\text{O}_4$ spinel solid solution at 1300 K. The symbols \blacksquare , \blacktriangle , and \blacklozenge represent ionic fractions of Al^{3+} , Fe^{2+} , and Mg^{2+} , respectively, on the octahedral site. Ionic fractions of Al^{3+} , Fe^{2+} , and Mg^{2+} on the tetrahedral site are represented by \square , \triangle , and \diamond , respectively.

Mixing on each cation sublattice is assumed to be ideal, and activities are represented by ionic fractions following Temkin's rule. The term $(-RT \ln 3)$ on the right-hand side of Eq. [14] represents the entropy contribution associated with randomization of Jahn–Teller distortion of the Fe^{2+} ion present on the tetrahedral site of the cubic spinel.^[20] Comparison of the measured cation distribution with that given by Eq. [14] is shown in Figure 5. For a spinel compound, it is sufficient to specify the ionic fraction of one cation on either tetrahedral or octahedral site. All other ionic fractions

are defined by mass and site balance. Experimental data are adequately represented by Eq. [14].

For the stoichiometric spinel solid solution $\text{Fe}_x\text{Mg}_{1-x}\text{Al}_2\text{O}_4$, the following mass balance relations can be written:

$$2 [N_{\text{Al}^{3+}}] + (N_{\text{Al}^{3+}}) = 2 \quad [15]$$

$$2 [N_{\text{Fe}^{2+}}] + (N_{\text{Fe}^{2+}}) = X \quad [16]$$

$$2 [N_{\text{Mg}^{2+}}] + (N_{\text{Mg}^{2+}}) = 1 - X \quad [17]$$

In addition, the sum of ionic fractions on each site must be unity:

$$\sum_i (N_i) = 1 \text{ and } \sum_j [N_j] = 1 \quad [18]$$

Combining ion exchange equilibria represented by Eqs. [12] and [14] with mass and site balance (Eqs. [15] through [18]), the cation distribution for the stoichiometric FeAl_2O_4 - MgAl_2O_4 solid solution was computed at 1300 K using MATLAB. Similar computations have been carried out earlier for other spinel solid solutions.^[21,22] The results are summarized in Table II. The variation of cationic fractions in tetrahedral and octahedral sites with spinel composition is illustrated in Figure 6.

Activities in the spinel solid solution can be calculated from the cation distribution:^[10]

$$a_{\text{FeAl}_2\text{O}_4} = \frac{(N_{\text{Fe}^{2+}})[N_{\text{Al}^{3+}}]^2}{(N_{\text{Fe}^{2+}}^o)[N_{\text{Al}^{3+}}^o]^2} \quad [19]$$

$$a_{\text{MgAl}_2\text{O}_4} = \frac{(N_{\text{Mg}^{2+}})[N_{\text{Al}^{3+}}]^2}{(N_{\text{Mg}^{2+}}^o)[N_{\text{Al}^{3+}}^o]^2} \quad [20]$$

where N_i^o represents the ionic fractions in pure spinels FeAl_2O_4 and MgAl_2O_4 , respectively. The computed activities given in Table II are almost ideal, with very small negative deviations from Raoult's law.

The experimental and theoretical free energies of mixing are compared in Figure 7. The measured values correspond to alumina-saturated compositions, while the theoretical curve corresponds to stoichiometric spinel solid solution. Variation of the small alumina solubility in the spinel solution with composition (X) is expected to lead to a slightly lower activity for ferrous aluminate, while the slight mis-

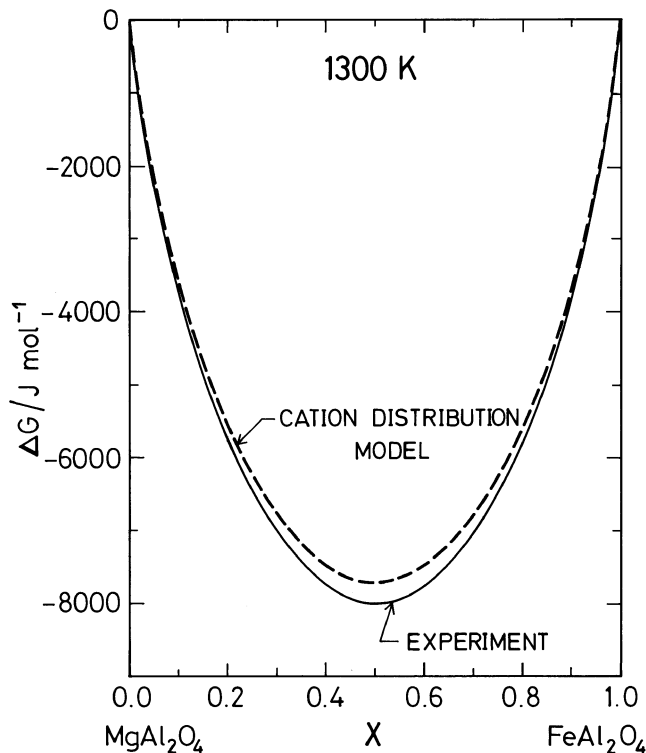


Fig. 7—Comparison of measured and computed free energies of mixing for the spinel solid solution at 1300 K.

match in ionic radii between Fe^{2+} (0.063 nm) and Mg^{2+} (0.057 nm) in fourfold coordination^[23] makes a small positive contribution to the energetics of mixing.^[10,21,22]

V. DISCUSSION

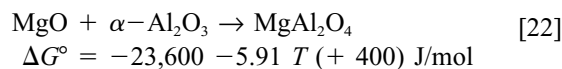
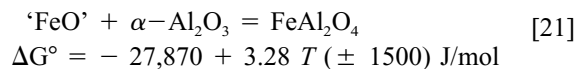
When the spinel phase is not saturated with respect to alumina, the oxygen potential at the electrodes of the solid state cell is not buffered by three-phase equilibria. The emf with unbuffered electrodes was found to drift with time, probably as a result of small oxygen exchange with the inert gas or electrochemical flux of oxygen through the solid electrolyte. While the composition of the spinel solid solution will shift to higher X values along the alumina-saturated curve, if oxygen is picked up by the three-phase electrode, the shift of composition of spinel phase in unsaturated electrodes will be toward the phase boundary composition in equilibrium with the monoxide solid solution $\text{Fe}_y\text{Mg}_z\text{O}$. Attempts are being made to improve the emf technique by encapsulating the electrode containing the spinel solid solution to prevent possible small oxygen exchange with the surroundings during experiments. It may then be possible to measure the activity of FeAl_2O_4 and MgAl_2O_4 as a function of $\text{MO}:\text{Al}_2\text{O}_3$ ratio, especially at higher temperatures, where nonstoichiometry of the spinel solid solution becomes significant.

Rosen and Muan^[24] have determined the tie-lines between spinel and monoxide solid solutions in the system $\text{CoO-MgO-Al}_2\text{O}_3$. From the phase equilibrium data and assuming ideal mixing in the monoxide phase,^[25] activities in the $\text{CoAl}_2\text{O}_4\text{-MgAl}_2\text{O}_4$ system were found to be approximately ideal. Cobalt aluminate is a normal spinel at low

temperature and the $\text{CoAl}_2\text{O}_4\text{-MgAl}_2\text{O}_4$ system is similar to the $\text{FeAl}_2\text{O}_4\text{-MgAl}_2\text{O}_4$ solid solution with respect to cation distribution. The close similarity in activity data for the two systems thus confirms theoretical expectations. Nickel aluminate (NiAl_2O_4) is an inverse spinel at low temperatures, and therefore, cation distribution in the $\text{NiAl}_2\text{O}_4\text{-MgAl}_2\text{O}_4$ solid solution changes dramatically with composition, giving rise to strong negative deviations from ideality.^[21] It thus appears that when the size differences of ions are not very different, mixing of two normal spinels is close to ideal, whereas negative deviations are expected when an inverse spinel is mixed with a normal spinel. These conclusions follow from a simple cation distribution model, in which site preference energies of cations are independent of composition, and cations are assumed to be randomly distributed on each cation sublattice. More complicated models^[15,16] with linear or quadratic dependence of site preference energies with composition or nonideal mixing on cation sublattices can give different results. Experimental studies on more spinel solid solution systems are needed to generalize their mixing behavior.

VI. PHASE EQUILIBRIA IN THE SYSTEM $\text{FeO-MgO-Al}_2\text{O}_3$

Phase relations in the $\text{FeO-MgO-Al}_2\text{O}_3$ system can be derived from activities in the spinel solid solution measured in this study and data on activities in FeO-MgO solid solution and Gibbs energies of formation of FeAl_2O_4 reported in the literature. There are four sets of activity data^[26-29] for the solid solution with rock salt structure. Although the results differ slightly, they all show positive deviation from ideality with a mean value of $W = \Delta G^E / X_{\text{FeO}}X_{\text{MgO}} = 10.46 (\pm 4)$ kJ/mol. The standard free energies of formation of pure spinels from component oxides can be represented by the following expressions:^[30,31]



The directions of conjugate lines between 'FeO'-MgO solid solution and spinel solid solution ($\text{FeAl}_2\text{O}_4 - \text{MgAl}_2\text{O}_4$) can be deduced from the equilibrium constant for intercrystalline ion exchange reaction between the two phases:



$$K_{(1300 \text{ K})} = \frac{a_{\text{MgO}} a_{\text{FeAl}_2\text{O}_4}}{a_{\text{FeO}} a_{\text{MgAl}_2\text{O}_4}} = 0.4915$$

For any chosen composition of the spinel solid solution, the ratio of activities in the spinel phase is known from the results of the present study. Although strictly these activities are measured along the Al_2O_3 -saturated compositions, they are not expected to change significantly since the width of the spinel solid solution field at 1300 K is very narrow. The activities in the spinel solid solutions are related to intracrystalline ion exchange between tetrahedral and octahedral sites, as discussed in Section IV. From Eq. [23], the activity ratio in the coexisting monoxide solid so-

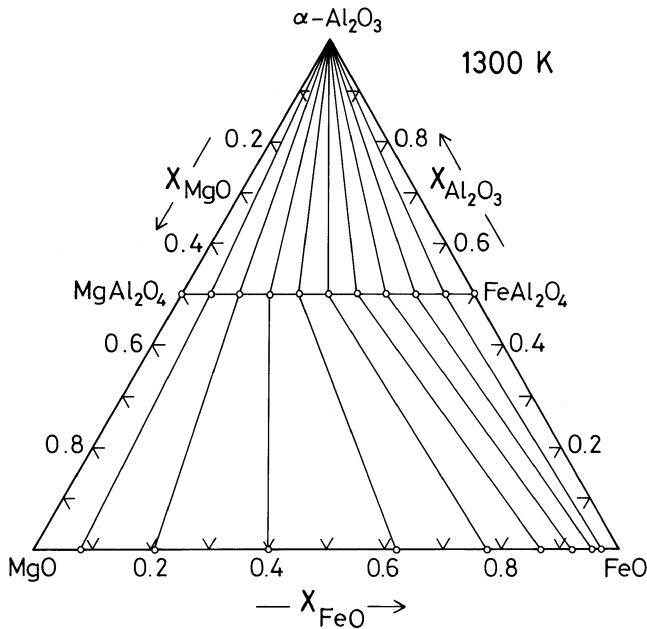


Fig. 8—Computed isothermal section of the 'FeO'-MgO-Al₂O₃ phase diagram at 1300 K.

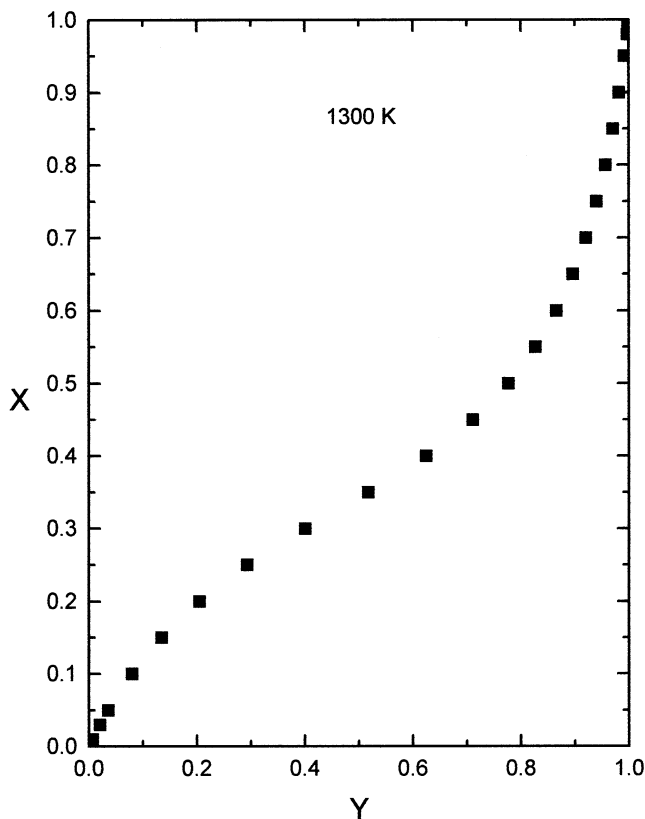


Fig. 9—Equilibrium relation between X (representing the mole fraction of FeAl₂O₄ in the spinel solid solution) and Y (denoting the mole fraction of FeO in the monoxide solid solution) at 1300 K.

lution can be evaluated. Since the activity-composition relationship in the monoxide solid solution is known,^[26-29] its equilibrium composition can be readily calculated. The tie-line results are shown in Figure 8. If the oxygen partial pressure over an equilibrium phase mixture Fe_YMg_{1-Y}O +

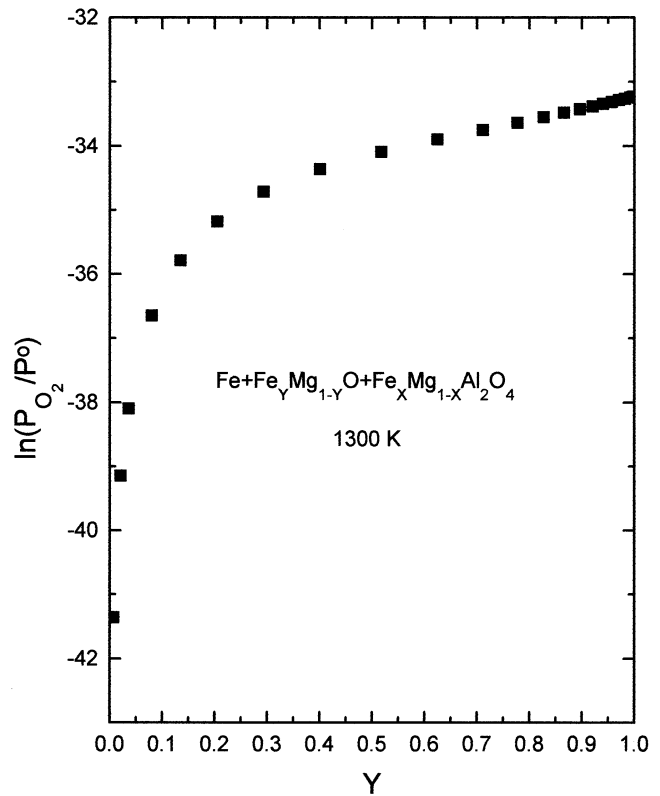
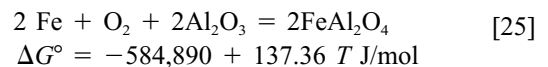
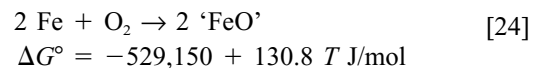


Fig. 10—Composition dependence of oxygen partial pressure corresponding to the three-phase equilibrium, Fe + Fe_YMg_{1-Y}O + Fe_XMg_{1-X}Al₂O₄, at 1300 K. The term P^o is the standard atmospheric pressure.

Fe_XMg_{1-X}Al₂O₄ is reduced below a critical value, the oxide mixtures will begin to decompose with the formation of metallic iron. Oxygen will be lost simultaneously from both oxide phases, making the solid solutions richer in MgO and MgAl₂O₄, respectively. The oxygen partial pressures are calculated from the following Gibbs energy changes:^[30,32]



The computed phase relations shown in Figure 8 require experimental confirmation. The dependence of X , representing the composition of the spinel solid solution, on Y , denoting the composition of the monoxide solid solution, at 1300 K is shown in Figure 9. The calculation demonstrates the effect of intracrystalline ion exchange equilibrium between crystallographically nonequivalent sites of the spinel structure on intercrystalline ion exchange equilibrium between phases (tie-lines). The composition dependence of oxygen partial pressure corresponding to the three-phase equilibrium, Fe + Fe_YMg_{1-Y}O + Fe_XMg_{1-X}Al₂O₄, at 1300 K is displayed in Figure 10. The oxygen potential for the three-phase equilibrium Fe + Fe_XMg_{1-X}Al₂O₃ + α -Al₂O₃ can be computed as a function of temperature from the emf of the solid-state cell and Eq. [25], which gives the oxygen potential involving pure hercynite. The composition dependence of the oxygen poten-

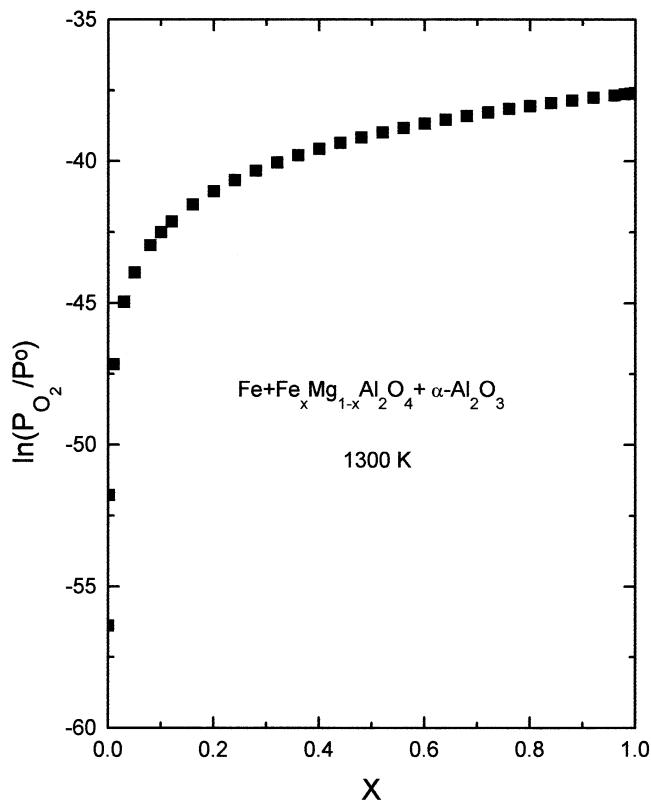


Fig. 11—Composition dependence of the oxygen partial pressure at 1300 K for the three-phase equilibrium, Fe + Fe_xMg_{1-x}Al₂O₄ + α-Al₂O₃.

tial at 1300 K is shown in Figure 11. Spinel solid solution is in equilibrium with metallic Fe for oxygen potentials that lie between the two three-phase equilibria displayed in Figures 10 and 11.

VII. CONCLUSIONS

Activities of both components in the spinel solid solution Fe_xMg_{1-x}Al₂O₄ exhibit mild negative deviations from Raoult's law. The mixing properties are adequately represented by a regular solution model:

$$\Delta H = \Delta G^E = -1990 X(1 - X) \text{ J/mol}$$

A theoretical analysis of cation distribution between tetrahedral and octahedral sites of the spinel supports the experimental results. The isothermal section of the phase diagram for the system FeO-MgO-Al₂O₃ at 1300 K is computed. The tie-lines between the monoxide and spinel solid solutions are mildly asymmetric and incline toward MgAl₂O₄. The oxygen partial pressures for three-phase equilibrium involving the solid solutions Fe₇Mg_{1-y}O and Fe_xMg_{1-x}Al₂O₄ are computed as a function of composition using activities measured in this study and auxiliary data from the literature.

ACKNOWLEDGMENTS

One of the authors (RP) expresses her gratitude to the Indian Academy of Sciences (Bangalore) for the grant of summer fellowships to conduct research at the Indian Institute of Science as part of the Academy Initiative in University Education. The authors are grateful to Ms. S. Yeshoda for assistance in the preparation of the manuscript.

REFERENCES

1. W.A. Deer, R.A. Howie, and J. Zussman: *Rock-Forming Minerals*, Longman Press, London, 1986, vol. 1 to 5.
2. F. Zambonini and G. Carobbi: *Boll. Soc. Nat. Napoli*, 1979, vol. 41, p. 245.
3. D.P. Serdyuchenko and V.A. Moleva: *Dokd. Acad. Sci. USSR*, 1973, vol. 88, p. 547.
4. F.H. Stewart: *Mineral Mag.*, 1942, vol. 36, pp. 260-66.
5. R.A. Binns: *Am. J. Sci.*, 1969, vol. 267A, pp. 33-49.
6. R.A. Binns, M.B. Duggan, and J.F.G. Wilkinson: *Am. J. Sci.*, 1970, vol. 269, pp. 132-68.
7. I. Kushiro and H.S. Yoder: *J. Petrol.*, 1966, vol. 7, pp. 337-62.
8. J.F.G. Wilkinson: *Contrib. Mineral. Petrol.*, 1957, vol. 53, p. 71.
9. S.E. Haggerty: in *Oxide Minerals*, D. Rumble III, ed., Mineralogical Society of America, 1976, pp. Hg 101-300.
10. A. Petric and K.T. Jacob: *Solid State Ionics*, 1982, vol. 6, pp. 47-56.
11. K.T. Jacob and C.B. Alcock: *Metall. Trans. B*, 1975, vol. 6B, pp. 215-21.
12. B.J. Wood, R.J. Kirkpatrick, and B. Montez: *Am. Mineral.*, 1986, vol. 71, pp. 999-1006.
13. R.L. Millard, R.C. Peterson, and B.K. Hunter: *Am. Mineral.*, 1992, vol. 77, pp. 44-52.
14. R.C. Peterson, G.A. Lager, and R.L. Hitterman: *Am. Mineral.*, 1991, vol. 76, pp. 1455-58.
15. H.S.C. O'Neill and A. Navrotsky: *Am. Mineral.*, 1983, vol. 68, pp. 181-94.
16. G.N.K. Iyengar, R. Balasubramanya, and K.T. Jacob: *High Temp. Mater. Process.*, 1997, vol. 16, pp. 39-48.
17. L. Larsson, H.S.C. O'Neill and H. Annersten: *Eur. J. Mineral.*, 1994, vol. 6, pp. 39-51.
18. R.J. Hill: *Am. Mineral.*, 1984, vol. 69, pp. 937-42.
19. S.B. Bohlen, W.A. Dollase, and V.J. Wall: *J. Petrol.*, 1986, vol. 27, pp. 1143-56.
20. T. Mathews and K.T. Jacob: *Solid State Commun.*, 1992, vol. 84, pp. 975-78.
21. K.T. Jacob and C.B. Alcock: *J. Solid State Chem.*, 1977, vol. 20, pp. 79-88.
22. A. Petric, K.T. Jacob and C.B. Alcock: *J. Am. Ceram. Soc.*, 1981, vol. 64, pp. 632-39.
23. R.D. Shannon: *Acta Crystallogr.*, 1976, vol. A32, pp. 751-67.
24. E. Rosen and A. Muan: *J. Am. Ceram. Soc.*, 1966, vol. 49, pp. 107-08.
25. E. Aukrust and A. Muan: *Trans. TMS-AIME*, 1963, vol. 227, pp. 1378-80.
26. W.C. Hahn, Jr. and A. Muan: *Trans. TMS-AIME*, 1962, vol. 224, pp. 416-20.
27. M.P. Morozova and G.P. Karlovskaya: *Zh. Fiz. Khim.*, 1960, vol. 34, pp. 117-21.
28. L.G. Schmahl, B. Frisch, and G. Stock: *Arch. Eisenhüttenwes.*, 1961, vol. 32, pp. 413-20.
29. A.V. Shashkina and Y.I. Gerasimov: *Zh. Fiz. Khim.*, 1953, vol. 27, p. 399.
30. J.C. Chan, C.B. Alcock, and K.T. Jacob: *Can. Metall. Qt.*, 1973, vol. 12, pp. 439-43.
31. K.T. Jacob, K.P. Jayadevan, and Y. Waseda: *J. Am. Ceram. Soc.*, 1998, vol. 81, pp. 209-12.
32. B.C.H. Steele: in *Electromotive Force Measurements in High-Temperature System*, C.B. Alcock, ed., The Institution of Mining and Metallurgy, London, 1968, pp. 3-25.